Arctic Ocean-Sea Ice Interactions

Greg Foss[a], An Nguyen[b], Victor Ocaña[b], Arash Bigdeli[b], Briana Bradshaw[a], Patrick Heimbach[b,c,d]

[a]*Texas Advanced Computing Center, The University of Texas at Austin, 10100 Burnet Road, Austin, TX 78758, USA*
[b]*The Institute for Computational Engineering and Sciences, The University of Texas at Austin, 201 E 24th St, Austin, TX 78712, USA*
[c]*The Institute for Geophysics, The University of Texas at Austin, Building 196 10100 Burnet Road, Austin, TX 78758, USA*
[d]*The Jackson School of Geosciences, The University of Texas at Austin, 2305 Speedway, Austin, TX 78712, USA*

Abstract

The Arctic Ocean, the smallest and shallowest of the five major oceans, is a unique physical and ecological system. With the recent shifts in global climate, which are amplified in the Arctic, this system is undergoing profound changes. Scientists are working to document these changes to provide a broad assessment of their local and global impact. The hostile environment makes comprehensive measurements challenging, calling for simulation-based science to support quantitative understanding. A critical element of simulation is visualizing the complex time-evolving three-dimensional ocean state. The showcased animation, created at the Texas Advanced Computing Center , University of Texas at Austin (UT), visualizes results of a high-resolution data-constrained numerical simulation of the circulation of the Arctic Ocean. Different view angles and zooms highlight emergent features, key to understanding some of the Arctic Ocean's most important processes.

The visualization serves as a public-outreach component of an NSF-funded project aimed at understanding and quantifying the Arctic ocean-sea ice mean state and its changes in response to the Earth's recent warming. The research is carried out at The Institute for Computational Engineering and Sciences, the Institute for Geophysics, and the Jackson School of Geosciences, UT. This paper describes briefly the science behind the simulation, the HPC requirements for running the high-resolution model simulation, and the iterative and evolving process of creating the animation. An HD version of the animation is currently being shown at the exhibition "Exploring the Arctic Ocean", which runs at the UT Visual Arts Center in Austin through the fall 2018 semester.

Keywords: scientific visualization, high performance computing, Arctic Ocean, polar climate, geophysical fluid dynamics, ocean general circulation, ocean modeling

1. Introduction

Understanding the coupled Arctic ocean-sea ice system, it's mean state and temporal evolution is a high-priority activity in climate research [1, 2]. Because sea ice presents a formidable obstacle to conducting comprehensive and sustained measurements in the Arctic, numerical simulations based upon general circulation models play an important role at supporting scientific progress. This paper describes briefly the HPC requirements for conducting the high-resolution Arctic Ocean-Sea Ice simulation and the creative process to visualize the simulation results, i.e. model output in meaningful ways. The visualization seeks to capture important physical processes and aspires to engage the general public to facilitate the conversation on Arctic Ocean research.

The video animation [Figure 1] serves as prototype for an in-progress, high-definition (HD) rendered version that is being projected on a 15×10 feet wall at the Visual Arts Center (VAC), University of Texas at Austin (UT), in an exhibit during the fall semester of 2018 [3], as part of the public outreach component in a National Science Foundation funded project[4]. The exhibition, entitled "Exploring the Arctic Ocean", combines the numerical-simulation-derived rendered video with works by several visual artists, who use various media to focus on a range of Arctic-inspired visual experiences. This merger promotes a broader understanding of the interrelations between some key elements of the Arctic. The goal of the exhibit is to foster an understanding of the complex changes by which the remote and dynamic environment of the Arctic Ocean is currently being transformed.

2. Simulation

2.1. Regional, nested modeling

As part of an NSF-funded project to study the time-mean state of the Arctic ocean-sea ice system and its changes during the early 21st century, an estimate of the polar ocean-sea ice state is obtained by solving the equations of motion of a fluid on a rotating sphere using the Massachusetts Institute of Technology general circulation model (MITgcm) [5, 6]. These equations were coded in FORTRAN and the resulting code parallelized by means of domain-decomposition. The code is executed on a 1008-core cluster ("Sverdrup") in the Computational Research

Email addresses: foss@tacc.utexas.edu (Greg Foss), atnguyen@ices.utexas.edu (An Nguyen), vocana@ices.utexas.edu (Victor Ocaña), abigdeli@ices.utexas.edu (Arash Bigdeli), brianabradshaw2015@gmail.com (Briana Bradshaw), heimbach@utexas.edu (Patrick Heimbach)

in Ice and Oceans Group (CRIOS) at UT's Institute for Computational Engineering and Sciences (ICES).

What sets the NSF project apart from other Arctic Ocean simulations is the application of inverse methods to bring the simulated state into consistency with much of the available satellite and in-situ observations. The result is the medium resolution (14 km in the Arctic) "Arctic Subpolar Gyre sTate Estimate" (ASTE) [4]. The model-data synthesis is achieved via a least-squares fit based on a gradient-based iterative optimization [7]. The gradient of the model-data misfit with respect to uncertain initial conditions, surface forcings, and model parameters was computed via the adjoint of the MITgcm, which in turn was derived by means of algorithmic differentiation. The AD approach used here inherits the scalability of the forward model (see below). [8]. A quasi-Newton variable-storage method is used in the optimization of ASTE, requiring an order of 100 iterations and several thousands hours of computing time. The high-resolution (4 km in the Arctic) configuration described in this paper is nested within the ASTE domain, with initial and time-varying lateral boundary conditions, as well as the time-varying optimized atmospheric forcings and internal ocean mixing parameters obtained from ASTE.

2.2. Numerical configuration

The physical domain of the high-resolution simulation covers the entire Arctic Ocean, its surrounding marginal Seas (Bering, Kara, Barents, Greenland, Norwegian, Iceland, Labrador, Canadian Archipelago), and the entire North Atlantic Ocean northward of 5°N. The horizontal domain size is composed of 1080×4140 grid points, with horizontal grid spacing ranging from ∼3.5 km in the Arctic to ∼7 km in the North Atlantic. The ocean's 6500 m depth is represented by 90 vertical levels placed at depth-varying intervals, ranging from 1 m at the surface, to capture upper ocean physics with high fidelity, to 250 m at depth, to alleviate the computational cost.

2.3. Scalability and HPC requirements

Scalability of the simulation on HPC architectures is achieved through domain decomposition, by which the physical domain is decomposed into a large number of tiles, with each tile assigned to a core and efficient cross-tile communication. For the domain chosen, the model exhibits good scalability across a range of tile sizes chosen, requiring 4968 cores for 30×30-size tiles to 552 cores for 90×90-size tiles. Courant-Friedrichs-Lewy (CFL) criteria, derived from vertical ocean velocity and the minimum ∼1.5 m vertical spacing, and numerical requirements associated with hourly tidal forcing, constrain the time-stepping interval to 240 s. The underlying processors used here are Intel(R) Xeon(R) E5–2695 at 2.30 GHz, 35 MB L3 cache.

Through optimization of exchanges to eliminate solving for the equations over land, the CPU load requirement can be reduced by nearly 50%. The production of a 2002–2017 model simulation, using 45×36 tiles and outputting 3D fields of the ocean and sea ice state at daily average frequency, required approximately 1200 computing hours on 860 cores spreading over 31 28-core computing nodes. A special configuration was used to distribute the number of cores per node to accommodate the I/O load on the first CPU. The maximum memory load on the first node was 140 GB, which is 78% of the available resources. Hourly rate of tidal forcing, 6-hourly atmospheric forcing, and daily outputs of 2D and 3D ocean-sea ice state resulted in a maximum of 27,000 IOPS with MPI communication approximately 42% of the time, and a total of approximately 56 TB of model output being written to disk.

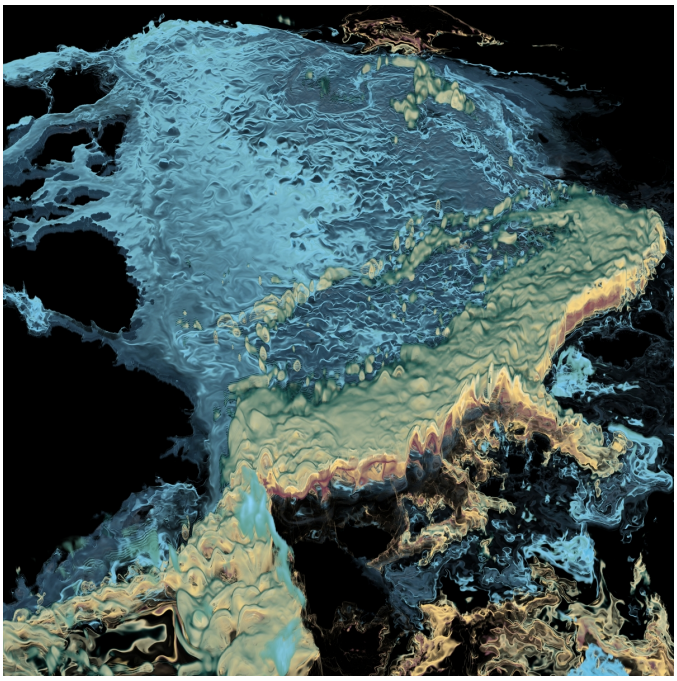

Figure 1: The sub-surface temperature of the Arctic Ocean, as viewed from the Greenland Sea. Red color shows the warm Atlantic Water current flowing eastward (counterclockwise) along the steep slope boundary of the Eastern Arctic basin. Yellow and green colors show colder temperature, with the gradation from yellow to green highlighting the mixing of temperature from the warm boundary current away from its source. Light and dark blue colors show coldest temperature within the Arctic Ocean interior.

3. Visualization

3.1. The Animation

The volume rendering, created with ParaView [9] and rendered with OSPRay[10], visualizes an Arctic Ocean simulation covering a eleven year period (2006–2016), with each frame (24 fps) showing a one day average. Warm green to yellow and red colors represent a temperature range from 1 to 2 °C, while light to dark blues show a range -1 to -2 °C. The video's opening map [Figure 2], based on the International Bathymetric Chart of the Arctic Ocean (IBCAO) Version 3.0 [11], positions the viewer above the North Pole, located at the center of the figure, looking directly down. The surrounding land areas are Svalbard at the bottom center, Greenland to the left, the Canadian Arctic Archipelago to the upper left, Alaska and the Bering Strait at the top, and then, moving clockwise, Siberia, Eurasia and northern Scandinavia on the right. The animation's slowly moving view gradually reveals a three dimensional domain spanning approximately 5200×3800 km^2, with depths between 0–800 meters.

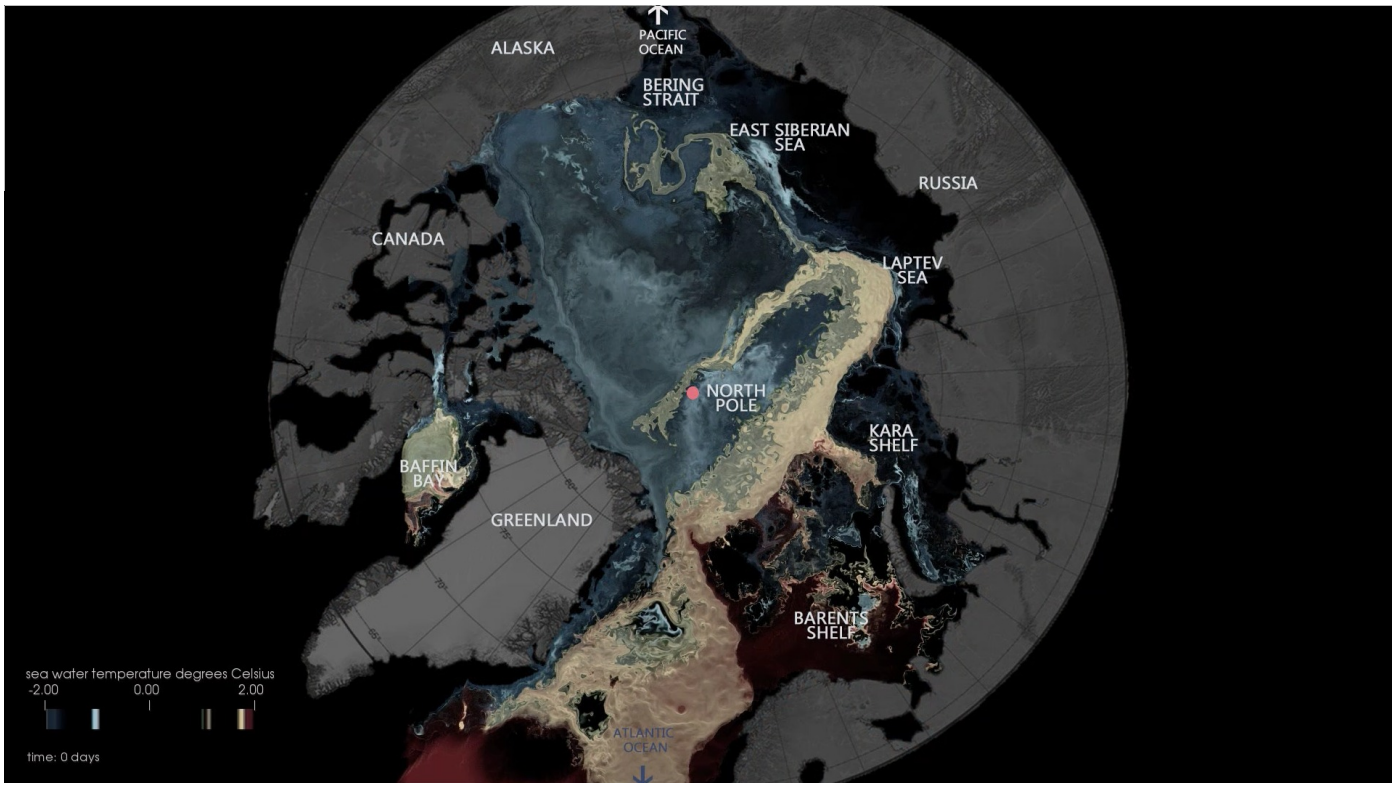

Figure 2: Video introduction orienting the viewer geographically.

3.2. The Data

While the full model state comprises several physical fields (temperature, salinity, 3-D velocity vector, sea surface elevation) spanning 4000 days we chose temperature as best representing the Arctic Ocean dynamics for the exhibition animation. The data was converted to VTK's[12] vti format for reading into ParaView[9] forming a regular 1500×1080×141 grid with nominal resolution 3.5×3.5 km^2 horizontally and 10 meters vertically (depth levels).

3.3. Color scale

The small range of temperatures and their very subtle gradation required extreme consideration in bringing forth different water masses and the turbulent nature of the flow in the Arctic Ocean interior. With the presence of sea ice, surface and near surface seawater is near its freezing temperature −2°C. In the Eastern Arctic, warm Atlantic Water (AW) with core average temperature of about 1.5°C resides at depths between 50 and 500 m. In the Western Arctic, this warm AW has core temperature in the range of 0.5–1°C and resides at depths between 200 and 700 m, with colder temperature of different origin residing above it. Thus, following a particular water mass requires knowledge of how this water has been mixed with its surrounding as well as where it resides in the water column based on its density.

The color scale chosen for the animation highlights four distinct ranges: (a) −2 to −1.75 °C , (b) −1.25 to −1 °C, (c) 1 to 1.25 °C, and (d) 1.6 to 2 °C. All other temperature ranges were made "transparent" to necessarily bring out the contrast. The warmest Atlantic Water in the Eastern Arctic, (range (d), [Figure 3]), is visualized using shades of bright yellow to dark red, with the warmest water seen flowing eastward (counterclockwise) along the Eastern Arctic basin boundary. The mixing of this warm water into the Eastern Arctic Basin interior can be seen in the gradation of color from bright yellow to dark green (range (c)). The usage of transparency between range (c) and (d), and between (b) and (c), allows the viewer to see isolated eddies being spun off from the main current and carrying the warm core temperature away from its source.

To follow this warm water layer into the Western Arctic would require a color range 0.5–1°C. However, if such color range is made opaque, it would mask out the warm core AW in the Eastern Arctic, as well as greatly diminish the ability to capture visually the individual eddies. Due to these subtle nuances, we opted to suppress this water mass (visually) in the Western Arctic and chose instead to highlight the colder layer (ranges (a) and (b)) residing vertically above it in the water column.

With this choice of color scale, only water within these featured temperature ranges can be seen, but not the water depth information. Knowledge of the Arctic Ocean is thus required to understand that the views presented here target iso-temperature-surfaces at depth. Finally, as temperature changes in the water column, e.g., from generally colder at surface to warmer at certain depth ranges to colder again at great depths, certain water-masses may be blocked if viewed from the top down or from bottom up. In this animation, we chose to exclusively view the water column from the top down, even at oblique angle.

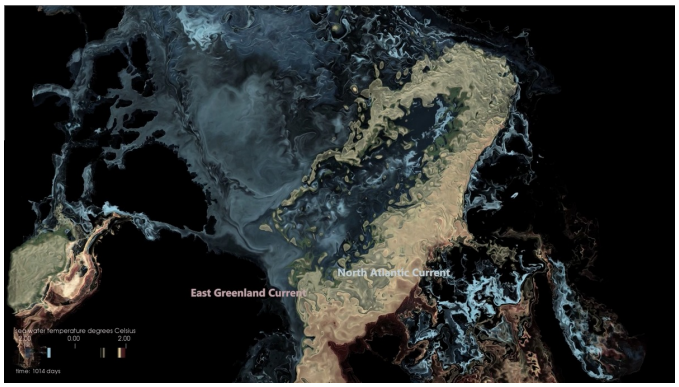

Figure 3: The Atlantic Water Current

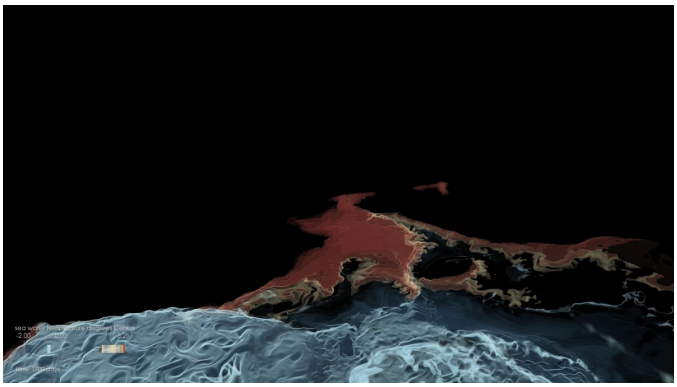

Figure 4: Bering Strait (center) warm Pacific (top of image) inflow

3.4. Visualization software

Visualization software ParaView[9] was selected for familiarity and available in-house support. One node running a single process on either TACC's Maverick[13] or Stampede2[14] systems ran a sufficiently stable gui. User interactivity was an important requirement of this project, due to a very narrow range of temperature values that demanded a fine manual selection of colors. Similarly, the presence of detailed physical structures required an interactive choice of camera angles and selections.

OSPRay [10] software rendering helped define clean outer edges, particularly among the more intricate and lacy outlying structures. Compared to ParaView's[9] default openGL rendering, OSPRay revealed considerably more detail, especially in the lower depths.

Finally Adobe Premier[15] was used to assemble the animation with gently drifting text labels, follwing, where appropriate, the adjacent current that they describe, and contributing to a sense of continuous motion.

A major challenge of this project arose, not so much from the technological side of producing the visualization, but rather from the exploration of such a complex and fascinating data set: sorting through a plethora of details and small-scale physical processes involved, experimenting with ever so slight adjustments in colors or domains to highlight the emerging features, and focusing on a set of dominant features to compose a narrative, required extensive interactions between scientists and members of TACC's Visualization Lab. Being able to explore this complex data set, with its intricate network of currents and swirling eddies, from close-up and far above, pushes the limits of creating a comprehensive visualization experience.

4. Scientific context

In the polar regions, where air temperature can drop significantly below -2°C (the freezing temperature for seawater), the sea surface freezes to form sea ice, and seawater just below the surface remains close to the freezing point. In this temperature range, the seawater density is controlled primarily by its salt content. Due to the difference in salt content, with Atlantic Water being saltier and heavier than Pacific Water, these two waters enter the Arctic at different depths. Atlantic Water circulates counter-clockwise (eastward) under the influence of the Coriolis force and steered by topographic features. As it enters the Western Arctic, Atlantic Water spreads *beneath* its Pacific counterpart, even though the latter is colder. It is only in the polar region that this curious phenomenon exists, whereby warmer water is stored at depth and is shielded from the surface sea ice by an in-between layer of colder and lighter water of Pacific origin. Scientists have observed a recent decrease in sea ice cover, warmer atmospheric temperatures, stronger surface winds over the Arctic region, and elevated ocean heat influx carried by the Atlantic-Norwegian Current into the Arctic Ocean [16, 17, 18]. Several key questions this project aims to address include to what extent the stronger winds may increase turbulent vertical mixing, erode the in-between cold buffering water layer, and potentially enable this Atlantic Water heat source to reach the surface and further melt sea ice [19]. Our visualization clearly highlights the warm-water pathways, and the mechanisms by which the ocean interior is filled through shedding of warm-water eddies. Quantification of these effects via salient metrics is a subsequent step, and is guided by the insights gained through the visualization. This research is on-going. It will require more dedicated visualization of the extensive diagnostic model output and in cross-sectional views. This, and the condensing of the complex information into key metrics that quantify the changes are beyond the scope of this paper.

The visualization thus serves to introduce the general public to the Arctic Ocean. This rendering of the model simulation shows the time-evolving ocean temperature, which highlights the circulation in the Arctic Ocean and its surrounding seas. In the following we briefly explain the main features of the simulation highlighted in the rendering.

Northward flow of Atlantic Water. The flow of Atlantic Water [Figure 3] originates from the Gulf Stream and extends via the North Atlantic Drift into the Nordic and Barents Seas, and further into the Arctic interior. This current may be viewed as the northern-most reach of the upper limb of the Atlantic Meridional Overturning Circulation (AMOC), a conceptualized view of the Atlantic circulation, by which warm, light waters are carried northward, overturn vertically, and return southward as cold, dense waters [20].

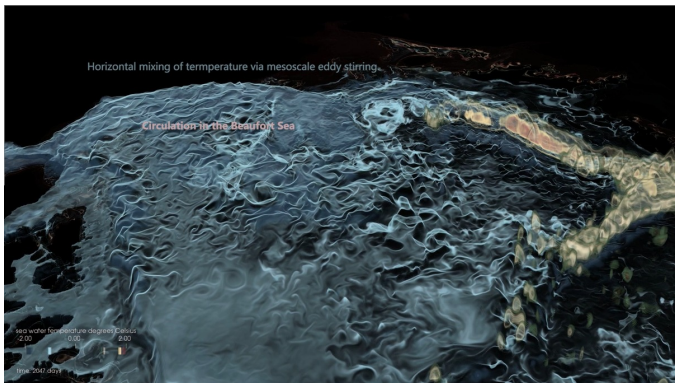

Figure 5: Circulation and eddie-stirring in the Beaufort Sea.

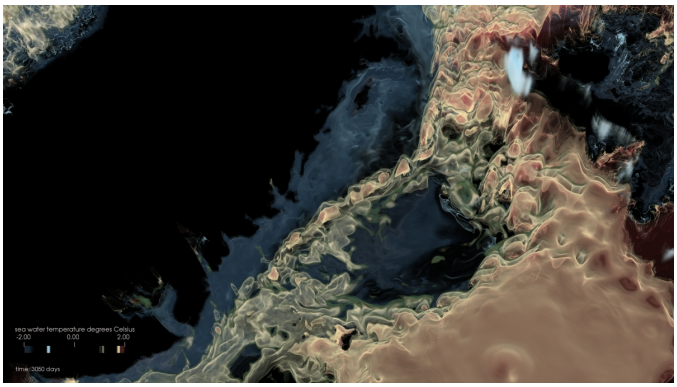

Figure 6: Greenland Sea, Greenland to the left. The Coriolis effect constrains warm water to the rim of the Greenland Sea Gyre (center).

Arctic Circumpolar Boundary Current. Warm Atlantic Water is shown flowing through the Norwegian-Greenland Seas [Figure 3, bottom of image] across Fram Strait into the Eastern Arctic. The flow continues as a boundary current flowing counterclockwise toward Siberia and into the Western Arctic, hugging the steep slope between the continental shelf and the deep Arctic interior [21]. Mesoscale eddies (the ocean's analogue of atmospheric storm systems), generated from the turbulent flow, extract heat from the main current and spread it into the Arctic Ocean interior at depths 50–700 m below the surface.

Bering Strait in the summertime. Throughout the year, water from the Pacific Ocean enters the Arctic through the Bering Strait [Figure 4, top of image]. This water is lighter (less dense) than its Atlantic counter-part, and thus resides at depths 0–250 m, which is above the Atlantic Water layer in the Western Arctic. During the summer months, Pacific-source water can have temperatures as high as 10°C [22]. In order to highlight the 'warm' water in the range 2–4 °C this segment of the visualization shows a temperature range extended up to 3.25°C (labeled on the color legend).

Circulation in the Beaufort Sea. In the Beaufort Sea, two circulation regimes dominate: a wind-driven clockwise circulation in the upper 200 m within the Beaufort Sea interior, and a counterclockwise circulation of the Atlantic Water current along the basin rim between 200–700 m. The clockwise circulation, typically strongest in the winter months, result in convergence of the fresher Pacific Water and sea ice melt in the Beaufort Sea [19, 23]. As the two circulation regimes and various water masses interact, mesoscale eddies of typical length-scales 1–15 km proliferate [Figure 5] throughout the basin interior. Through a mechanism termed "eddy-stirring", these eddies mix temperature and salinity and act to flatten out stratification.

Fram Strait and the East Greenland Current. The Fram Strait is one of the two major gateways through which Atlantic Water enters the Arctic Ocean [Figure 3]. Atlantic Water enters on the Svalbard side along the West Spitsbergen current at or near the surface [24]. Once inside the Arctic, due to the presence of sea ice and fresh water (in this context, "fresh" describes water with small salt content compared to typical sea water), Atlantic Water subducts below the fresh layer and occupies the Eastern Arctic at depths below 50 m. On the western side of Fram Strait (off Northeast Greenland), cold and fresh water (of Pacific-source, river runoff, and ice melt) exits near the surface as the East Greenland Current [Figure 3], and modified Atlantic Water exits at depth. The large velocity gradient at the strait (northward inflow and southward outflow) generates large numbers of mesoscale eddies.

Greenland Sea. The Greenland/Iceland/Norwegian (GIN, [Figure 6]) and Labrador Seas are key regions of weak stratification (well mixed and with only small vertical density gradients) where surface water loses heat to the cold winter-time surface atmosphere, leading to convective mixing and deep water formation that supplies the deep southward return flows [25].

Kangerdlugssuaq Fjord and outlet glacier. The last feature labeled in the video shows oceanic heat transport toward the Greenland ice sheet's marine margin in Kangerdlugssuaq Fjord. [Figure 7] Through narrow, deep fjords such as this one, interactions take place between the ocean and the Greenland Ice Sheet. Warm subsurface Atlantic water can penetrate to the base of Greenland outlet glaciers and enhance glacial melting, contributing to the observed recent (since the late 1990s) accelerated Greenland ice mass loss [26] .

5. Summary

Key features of the Arctic and subpolar North Atlantic Ocean circulation are intense, narrow boundary currents and mesoscale eddies of sizes less than 15 km (they are the oceans analogue of synoptic-scale atmospheric disturbances of order 1000 km), all of which transport and redistribute heat and freshwater. Capturing these features is key for faithfully representing the time-evolving Arctic coupled atmosphere-ocean-cryosphere system and its role in climate variability and change. Such representation in models is impossible without high performance computing resources. Advanced visualization of these complex and vast data sets leads to rapid progress in process understanding.

With the recent observed drastic increase in atmospheric temperatures (Arctic amplification), increased mass loss of the

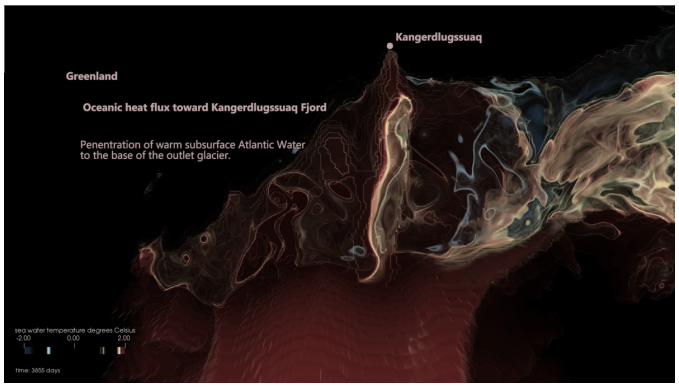

Figure 7: Kangerdlugssuaq Fjord

Greenland ice sheet and Arctic glaciers, and decrease in Arctic summertime sea ice coverage, improved understanding and quantification of how heat and freshwater are transported by the ocean currents will be essential to assess the impact of these changes on the Arctic climate system, on Greenlands contribution to global sea level rise, and the wider implications for the global climate system as a whole.

Acknowledgments

A. Nguyen, A. Bigdeli, V. Ocaña, and P. Heimbach are supported in part by NSF OPP grant 1603903 and NASA PO ("Estimating the Circulation and Climate of the Ocean" via a JPL/Caltech subcontract). Many thanks to fellow TACC staff, especially Director of Visualization Paul Navrátil and Anne Bowen of the Scalable Visualization Technologies group, for their technical support and helpful advice.

References

[1] W. Maslowski, J. Perlwitz, D. Wuebbles, Arctic changes and their effects on alaska ans the rest of the united states, in: D. Wuebbles, D.J., D. Fahey, K. Hibbard, D. Dokken, B. Stewart, T. Maycock (Eds.), Climate Science Special Report: Fourth National Climate Assessment, U.S. Global Change Research Program, 2017, Ch. 11, pp. 303–332.

[2] Arctic Research Consortium of the United States, Opportunities and challenges in arctic system synthesis, Consensus report, City University of New York, New York, NY (2018).

[3] A. T. Nguyen, G. Foss, V. Ocaña, P. Heimbach, U. Heine, Exploring the Arctic Ocean, Exhibit, Visual Arts Center, University of Texas at Austin (September–December 2018).
URL `http://exploringthearcticocean.org`

[4] A. T. Nguyen, V. Ocaña, V. Garg, P. Heimbach, J. Toole, R. Krishfield, On the benefit of current and future alps data for improving arctic coupled ocean-sea ice state estimation, Oceanography 30 (2) (2017) 69–73.
URL `http://doi.org/10.5670/oceanog.2017.223`

[5] J. Marshall, A. Adcroft, C. Hill, L. Perelman, C. Heisey, A finite-volume, incompressible Navier Stokes model for studies of the ocean on parallel computers, Journal of Geophysical Research 102 (1997) 5753–5766.

[6] A. Adcroft, C. Hill, J. M. Campin, J. Marshall, P. Heimbach, Overview of the formulation and numerics of the MIT GCM, in: ECMWF Conference Proceedings, ECMWF, Shinfield Park, Reading, UK, 2004, pp. 139–150.

[7] C. Wunsch, P. Heimbach, Dynamically and Kinematically Consistent Global Ocean Circulation and Ice State Estimates, in: Ocean Circulation and Climate: A 21st Century Perspective, Elsevier Ltd., 2013, pp. 553–579.

[8] P. Heimbach, C. Hill, R. Giering, An efficient exact adjoint of the parallel MIT General Circulation Model, generated via automatic differentiation, Future Generation Computer Systems 21 (8) (2005) 1356–1371.

[9] ParaView [online]. www.paraview.org [cited 2018].

[10] OSPRay [online]. www.ospray.org [cited 2018].

[11] M. Jakobsson, L. Mayer, B. Coakley, J. A. Dowdeswell, S. Forbes, B. Fridman, H. Hodnesdal, R. Noormets, R. Pedersen, M. Rebesco, H. W. Schenke, Y. Zarayskaya, D. Accettella, A. Armstrong, R. M. Anderson, P. Bienhoff, A. Camerlenghi, I. Church, M. Edwards, J. V. Gardner, J. K. Hall, B. Hell, O. Hestvik, Y. Kristoffersen, C. Marcussen, R. Mohammad, D. Mosher, S. V. Nghiem, M. T. Pedrosa, P. G. Travaglini, P. Weatherall, The International Bathymetric Chart of the Arctic Ocean (IBCAO) Version 3.0, Geophysical Research Letters 39 (12) (2012) n/a–n/a.

[12] VTK [online]. www.vtk.org [cited 2018].

[13] Maverick [online]. www.tacc.utexas.edu/systems/maverick [cited 2018].

[14] Stampede2 [online]. www.tacc.utexas.edu/systems/stampede2 [cited 2018].

[15] Adobe Premier [online]. www.adobe.com [cited 2018].

[16] I. V. Polyakov, A. V. Pnyushkov, M. B. Alkire, I. M. Ashik, T. M. Baumann, E. C. Carmack, I. Goszczko, J. Guthrie, V. V. Ivanov, T. Kanzow, R. Krishfield, R. Kwok, A. Sundfjord, J. Morison, R. Rember, A. Yulin, Greater role for Atlantic inflows on sea-ice loss in the Eurasian Basin of the Arctic Ocean, Science 356 (6335) (2017) 285–291.

[17] I. V. Polyakov, U. S. Bhatt, J. E. Walsh, E. P. Abrahamsen, A. V. Pnyushkov, Recent oceanic changes in the Arctic in the context of long-term observations, Ecological Applications 23 (8) (2013) 1745–1764.

[18] L. Rainville, C. Lee, R. Woodgate, Impact of wind-driven mixing in the Arctic Ocean, Oceanography 24 (3) (2011) 136–145. doi:http://dx.doi.org/10.5670/oceanog.2011.65.

[19] E. Carmack, I. Polyakov, L. Padman, I. Fer, E. Hunke, J. Hutchings, J. Jackson, D. Kelley, R. Kwok, C. Layton, H. Melling, D. Perovich, O. Persson, B. Ruddick, M. L. Timmermans, J. Toole, T. Ross, S. Vavrus, P. Winsor, Toward quantifying the increasing role of oceanic heat in sea ice loss in the new Arctic, Bulletin of the American Meteorological Society 96 (12) (2015) 2079–2105.

[20] M. S. Lozier, Overturning in the North Atlantic, Annual Review of Marine Science 4 (1) (2012) 291–315.

[21] Y. Aksenov, V. V. Ivanov, A. J. G. Nurser, S. Bacon, I. V. Polyakov, A. C. Coward, A. C. Naveira Garabato, A. Beszczynska-Moeller, The Arctic Circumpolar Boundary Current, Journal of Geophysical Research 116 (C9) (2011) C09017.

[22] R. A. Woodgate, Increases in the Pacific inflow to the Arctic from 1990 to 2015, and insights into seasonal trends and driving mechanisms from year-round Bering Strait mooring data, Progress in Oceanography 160 (2018) 124–154.

[23] A. Proshutinsky, D. Dukhovskoy, M.-L. Timmermans, R. Krishfield, J. Bamber, Arctic circulation regimes., Philosophical Transactions of the Royal Society of London. Series A: Mathematical, Physical and Engineering Sciences 373 (20140160). doi:http://dx.doi.org/10.1098/rsta.2014.0160.

[24] B. Rudels, M. Korhonen, U. Schauer, S. Pisarev, B. Rabe, A. Wisotzki, Circulation and transformation of Atlantic water in the Eurasian Basin and the contribution of the Fram Strait inflow branch to the Arctic Ocean heat budget, Progress in Oceanography 132 (C) (2015) 128–152.

[25] B. Rudels, The thermohaline circulation of the Arctic Ocean and the Greenland Sea, Philosophical Transactions of the Royal Society of London. Series A: Physical and Engineering Sciences 352 (1699) (1995) 287–299.

[26] M. Inall, T. Murray, F. Cottier, K. Scharrer, T. Boyd, K. Heywood, S. Bevan, Oceanic heat delivery via kangerdlugssuaq fjord to the south-east greenland ice sheet, Journal of Geophysical Research:Oceans (119) (2014) 631–645.